Title
Feasibility study of normal and septic tracheal imaging using optical coherence tomography

Journal
Lasers in Surgery and Medicine, 35(2)

ISSN
0196-8092

Authors
Jung, Woonggyu
Zhang, Jun
Mina-Araghi, Reza
et al.

Publication Date
2004-08-01

DOI
10.1002/lsm.20072

Lasers in Surgery and Medicine 35:121–127 (2004)

Feasibility Study of Normal and Septic Tracheal Imaging Using Optical Coherence Tomography

Woonggyu Jung,[1,2] Jun Zhang,[1] Reza Mina-Araghi,[1,3] Nevine Hanna,[1] Matthew Brenner,[1,3] J. Stuart Nelson,[1,2,4] and Zhongping Chen, PhD[1,2]*

[1]*Beckman Laser Institute, University of California, Irvine, California 92612*
[2]*Department of Biomedical Engineering, University of California, Irvine, California 92697*
[3]*Department of Pulmonary Medicine, University of California, Irvine, California 92868*
[4]*Department of Surgery, University of California, Irvine, California 92868*

Background and Objectives: Optical coherence tomography (OCT) is an imaging technology that may be adapted for use with flexible fiberoptic bronchoscopy, potentially allowing it to play an important role in pulmonary diagnostics. The goal of this study was to evaluate the feasibility of OCT to image tracheal pathology.

Study Design/Materials and Methods: Tracheas were harvested from normal and septic New Zealand White rabbits and imaged using OCT. Two delivery devices were employed. One was a moving stage with an objective lens and collimator, the other a linear scanning flexible fiberoptic catheter using a GRIN lens and prism for endoscopic OCT. After OCT images were obtained from normal and septic tracheas, the excised tissues were prepared for standard histologic examination. Areas imaged by OCT were compared with corresponding histology slides.

Results: OCT images demonstrated in detail tracheal subsurface structures such as the epithelium, lamina propria, submucosa, and cartilage. The appearance of structures imaged by OCT corresponded very well with histologic pictures obtained by light microscopy. The OCT images from septic tracheas showed marked swelling of the mucosal and submucosal layers. Such pathology was equally imaged by either the moving stage or fiberoptic catheter for endoscopic OCT.

Conclusions: OCT images of the trachea can distinguish many sub-surface structural features usually requiring biopsy and light microscopy for visualization. Marked differences between normal and septic trachea were apparent in OCT images. In the future, OCT may be a valuable tool for evaluating tracheal pathology in situ with high image resolution. Lasers Surg. Med. 35:121–127, 2004.

Key words: optical coherence tomography; tracheal imaging; inflammation; pulmonary diagnostics; endoscopic optical coherence tomography

INTRODUCTION

Real-time, non-invasive, direct visualization of tissue anatomy provides important information for the diagnosis and clinical management of a wide range of diseases. Medical imaging technologies such as ultrasound, CT, and MRI have been used as pulmonary diagnostic tools, but have limited resolution for non-invasive or minimally invasive imaging. Improved imaging techniques are essential for more accurate diagnosis and staging of many diseases and would have a significant impact in biomedical research, clinical diagnostics, and treatment.

Optical coherence tomography (OCT) is an evolving imaging modality used to obtain high-resolution, high-speed, non-invasive or minimally invasive endoscopic imaging of superficial tissues [1–3]. Frequently, OCT is compared with ultrasound because both technologies employ back-scattered signals reflected from different layers within the tissue to reconstruct structural images. OCT is based on the detection of light waves rather than sound, which enables resolution in the range of 2–10 μm with near real-time image acquisition.

The most extensive clinical use of OCT has been in the field of ophthalmology. The eye provides a uniquely suitable medium for OCT retinal imaging due to its transparent nature, minimal optical scattering, and excellent light penetration [4]. The ability of OCT to be incorporated into flexible fiberoptic probes has broadened the range of endoscopic imaging to gastroenterology, cardiology, and urology [5–10]. Fiberoptic capabilities enable in situ imaging of virtually any organ accessible by a catheter or endoscope. In pulmonary medicine, endoscopic tools such

Contract grant sponsor: National Science Foundation; Contract grant number: BES-86924; Contract grant sponsor: California Tobacco Related Disease Research Program; Contract grant number: 6RT-0158; Contract grant sponsor: National Institutes of Health; Contract grant numbers: AR47551, EB-002SS, EB-00293, EB-002495, NCI-91717, RR-01192; Contract grant sponsor: Philip Morris External Research Program; Contract grant number: PMUSA-32598; Contract grant sponsor: Air Force Office of Scientific Research; Contract grant number: F49620-00-1-0371; Contract grant sponsor: Beckman Laser Institute Endowment.
*Correspondence to: Zhongping Chen, PhD, Beckman Laser Institute, 1002 Health Sciences Road East, Irvine, CA 92612-1475. E-mail: zchen@laser.bli.uci.edu
Accepted 20 April 2004
Published online in Wiley InterScience (www.interscience.wiley.com).
DOI 10.1002/lsm.20072

as flexible bronchoscopy are a mainstay of diagnostics and therapeutics for endobronchial diseases including inflammatory conditions, malignancy, and infections.

The purpose of this study was to evaluate the feasibility of OCT for high-resolution imaging of normal and septic tracheas. Imaging using a moving stage and a fiber based endoscopic catheter was investigated to demonstrate OCT capabilities in the upper airway under simulated clinical conditions.

MATERIALS AND METHODS

Sample Preparation

Two groups of tracheas were imaged from normal and septic New Zealand White (NZW) rabbits. For the normal group, rabbits were sacrificed and their tracheas removed and maintained in cold isotonic saline until imaged using OCT. No tracheal abnormalities occurred in these animals (as demonstrated in previous histologic evaluations). Samples were repeatedly imaged for up to 4 days post-sacrifice to verify maintenance of normal tissue structure during cold storage.

For the septic group, healthy NZW rabbits were sedated and intubated, and varying doses of *S. pneumoniae* were inoculated into each animal's airway through a sterile pediatric suction catheter (under an ARC approved protocol at the U.S. Army Institute of Surgical Research, San Antonio, TX). The rabbits were subsequently extubated and monitored until the animals developed pneumonia and sepsis. Other diagnostic studies including airway lavage, chest X-ray, and laboratory data were used to confirm the progressive pneumonia and sepsis. At the end of the 4-day sepsis study period, animals were euthanized and the tracheas excised for OCT imaging with histological comparative studies. Normal and septic tracheas were maintained in cold saline and imaged within 4 days of tissue harvest.

OCT Instrumentation

A schematic of the OCT system is shown in Figure 1. A low-coherence length light source that delivered an output power of 10 mW at a central wavelength of 1,310 nm with a bandwidth of 70 nm was coupled into a fiber based Michelson interferometer. The scanning beam was directed towards the tissue in the sampling arm of the interferometer and a rapid-scanning optical delay line (RSOD) in the reference arm. A visible aiming beam (633 nm) was used to locate the exact position on the sample.

Two types of imaging delivery devices were employed in the scanning arm. One was a bench-top moving stage scanner with an objective lens and collimator, the other a linear scanning flexible fiberoptic catheter using a GRIN lens and prism for endoscopic OCT [1,11]. Both devices were launched from the moving stage and performed linear scanning at a speed of 5 mm/second [2]. The catheter consisted of three main components: single mode fiber, GRIN lens, and micro prism. A single mode fiber with a core diameter of 9 μm guided the light through the center of the endoscopic probe. The distal end was comprised of a 0.7 mm diameter, 0.2725 pitch GRIN lens, and a 0.5 mm right angle

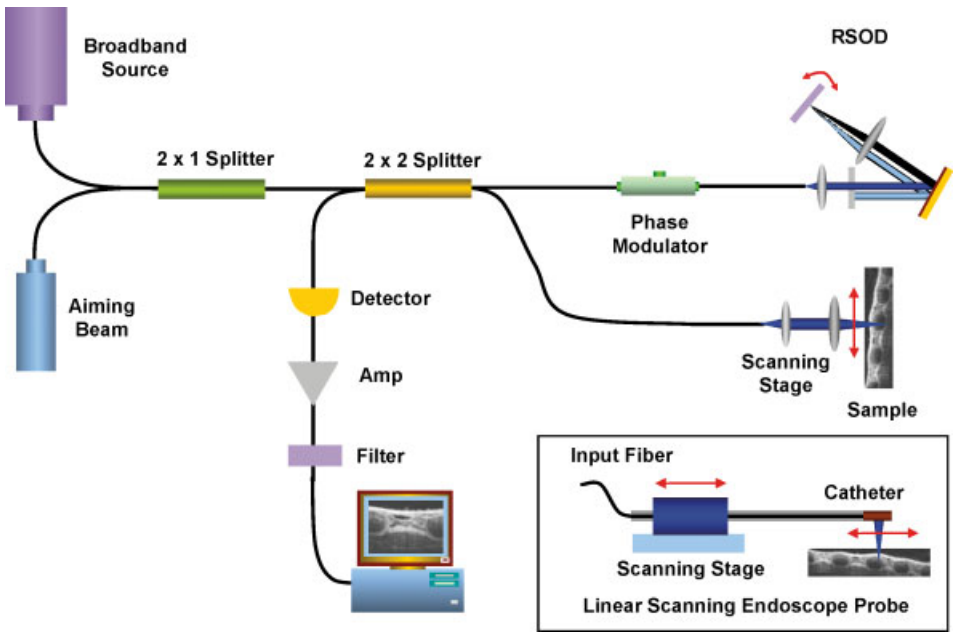

Fig. 1. Schematic of the optical coherence tomography (OCT) system. Two beam delivery devices were used: one is a bench-top moving stage scanner with objective lens and collimator, and the other a linear scanning flexible fiberoptic catheter with a GRIN lens and prism. Both systems were used to perform linear scanning; RSOD, rapid scanning optical delay. [Figure can be viewed in color online via www.interscience.wiley.com.]

micro prism. The outer diameter of the endoscopic probe was a 2 mm transparent window. The focal length of this probe was 2.5 mm. Spot sizes of the bench-top scanner and catheter were 10 and 45 μm, respectively.

In the reference arm, a RSOD was used that employed a grating to control the phase and group delays separately so that no phase modulation was generated when the group delay was scanned [12,13]. Phase modulation was generated through an electro-optic phase modulator that produces a carrier frequency. The axial line scanning rate was 400 Hz and the modulation frequency was 500 kHz.

Reflected beams from the two arms were recombined in the interferometer and detected with a photodetector. Interference signals were observed only when the optical path length difference of the two interferometer arms matched within the source coherence path length. The detected optical interference fringes intensity signals were filtered at the carrier frequency and resultant signals displayed as 2D images with 10 μm axial resolution after signal processing.

OCT Imaging

Tracheal samples were cut into sections approximately $1.5 \times 1.5\ cm^2$ in size and mounted on small cork-boards with the mucosal surface exposed. Triangular notches were cut at the edges of the trachea to mark the area to be imaged. Mucosal surfaces were gently rinsed with normal saline to remove any mucous and debris, and a thin layer of K-Y Jelly (Johnson & Johnson Products, Inc., NJ) was placed on the sample to prevent tissue desiccation while the OCT images were obtained.

Specimens were then placed on the sample platform and a visible-light guiding beam was used to match the line of image acquisition with the triangle notches. Images of various size and resolution were obtained by the fiber based OCT system and displayed using a logarithmic intensity scale.

After OCT imaging, tissues were placed in formalin and prepared for comparative histological examination. Tissues were cut into sections along the same line as the OCT image acquisition and stained with hematoxylin and eosin (H&E). The OCT images and corresponding histological preparations of normal and septic tracheal specimens were compared on the basis of the tissue morphology.

RESULTS

OCT images with 10 μm resolution, 1.3 mm axial by variable lengths from 2 to 14 mm in the horizontal direction were performed. Figure 2 shows a representative OCT image and the corresponding histology of a normal rabbit trachea. The OCT images corresponded very closely to the standard histological light microscopic pictures. Excellent resolution of tissue layers, structures, glands, membranes, and cartilage were obtained by OCT and easily recognizable due to their strong similarities with standard histology. Epithelium, mucosa, cartilage are clearly differentiated as well as a number of glandular tissues by both OCT (Fig. 2A) and histology (Fig. 2B). The similarity between the OCT image and the corresponding standard histologic image is readily apparent.

Figure 3A shows a 14 mm segment of normal rabbit trachea imaged by OCT. Figures 3B–F show higher magnification views of Figure 3A. As shown in Figure 3, cartilage, glandular structures, epithelial layers, and basement membranes are again clearly visualized, illustrating the resolution capabilities of OCT for tracheal mucosa and submucosa.

In Figure 4, OCT images of rabbit trachea exposed to nebulized pneumococcal bacteria with subsequent development of sepsis are shown. Bacterial exposure caused swelling of the mucosa and submucosa due to inflammation and edema, with increased thickening between the epithelial surface and cartilage, loss of submucosal glands and structural definition. These changes are evident throughout the entire tracheal image (Fig. 4A) and in the higher magnification views (Figs. 4B–E).

Figure 5 shows higher magnification views of the OCT images and comparison with standard histology. In contrast to normal trachea (Figs. 5A,B), mucosal and submucosal edema is observed in the septic tracheas by OCT (Fig. 5C) and histology (Fig. 5D). The septic tracheas showed marked edema and swelling of the submucosal

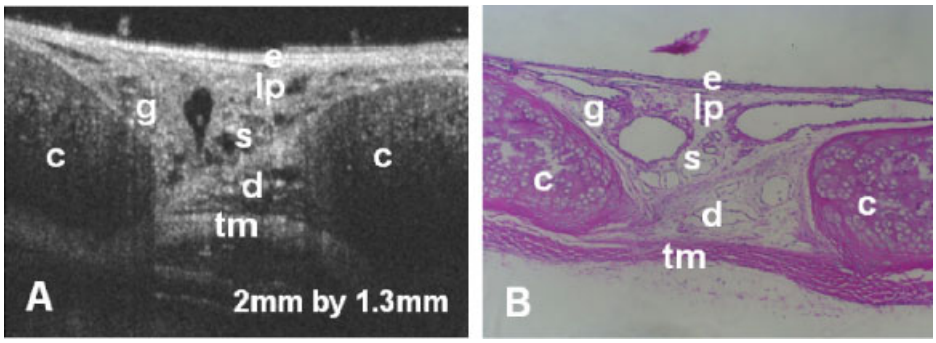

Fig. 2. Comparison between OCT (**A**) and H&E section (**B**) of normal rabbit trachea ($2 \times 1.3\ mm^2$, 10 μm/pixel): c, cartilage; e, epithelium; g, glands; lp, lamina propria; d, dense fibro elastic-tissue; s, submucosa; tm, tunica muscularis. [Figure can be viewed in color online via www.interscience.wiley.com.]

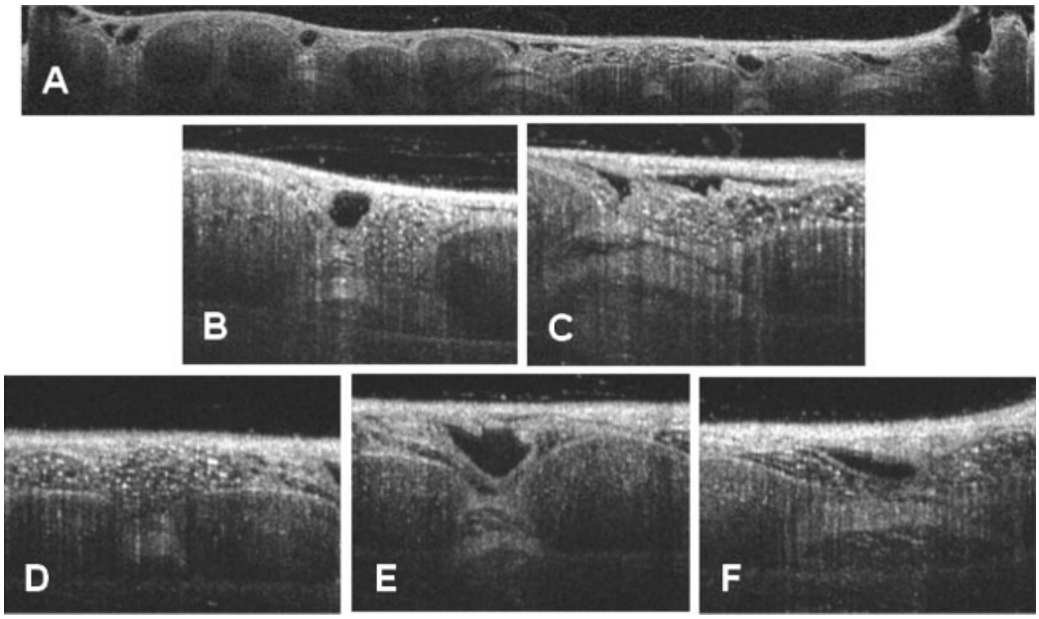

Fig. 3. Normal rabbit trachea OCT images: (**A**) a 14 mm segment of normal rabbit trachea imaged by OCT; (**B–F**) higher magnification views of (A). The size of the OCT images shown is 2×1.3 mm^2 with 10 μm/pixel display resolution.

region, with glandular structures less clearly visualized. Septic tracheas were easily distinguished from normal specimens due to these submucosal changes. Some edema was not readily apparent in the histologic sections due to tissue sample desiccation during H&E preparation.

Figure 6 presents in vitro endoscopic images of septic trachea obtained from an intubated rabbit acquired through an endotracheal tube. Epithelial, mucosal, and submucosal structures are seen. Figures 6A,B were obtained from septic trachea at different stages of infection.

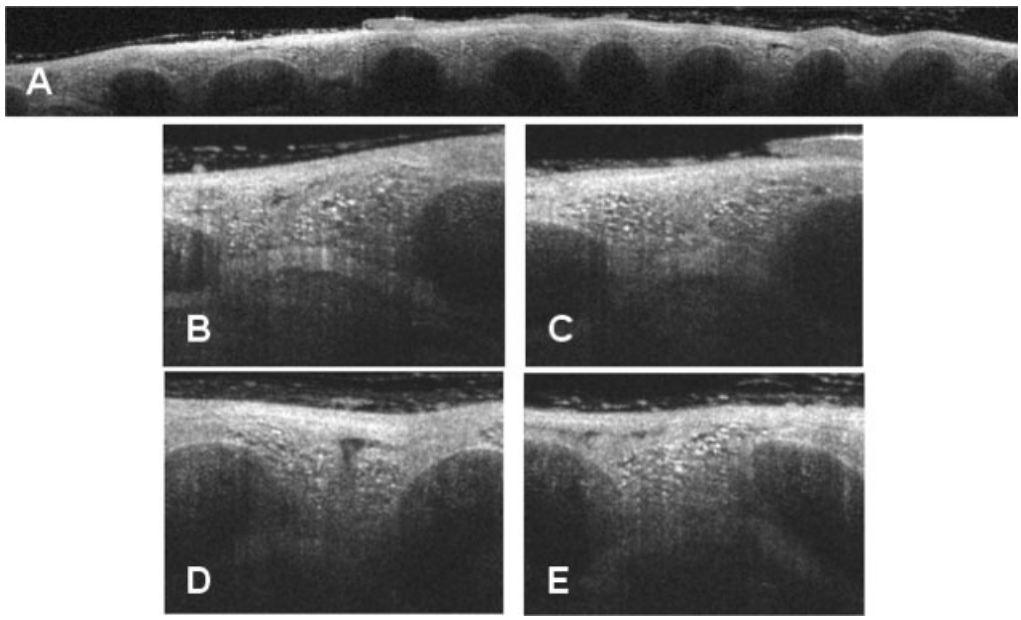

Fig. 4. Septic rabbit trachea OCT images: (**A**), a 14 mm segment of septic rabbit trachea imaged by OCT; (**B–E**) higher magnification views of (A). The size of OCT images is 2×1.3 mm^2 with 10 μm/pixel.

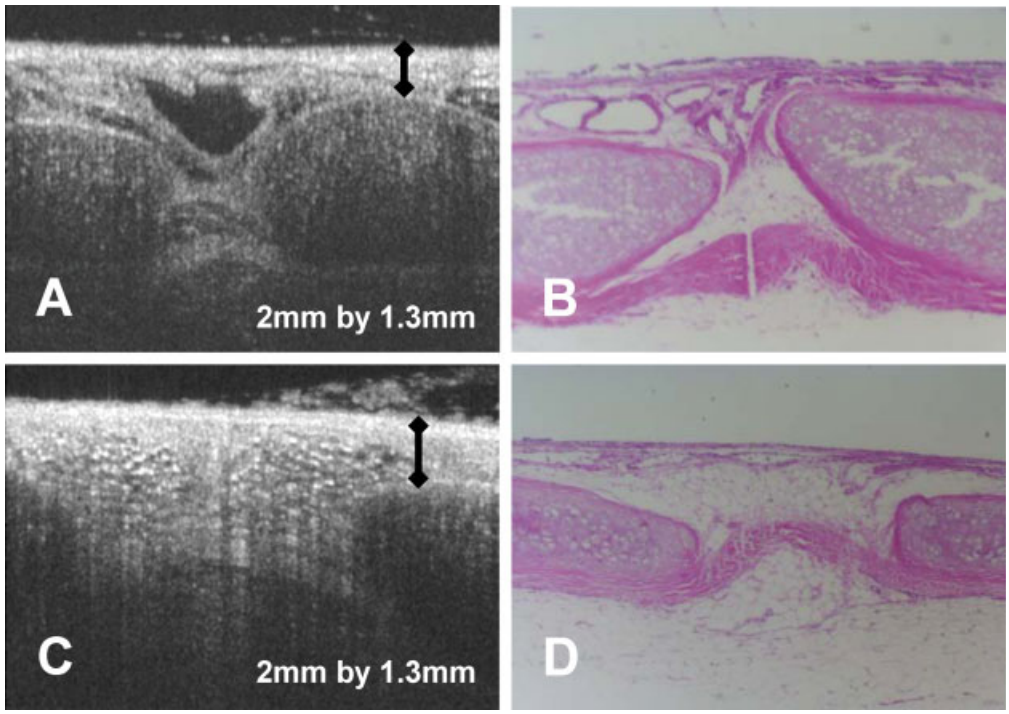

Fig. 5. Comparison between OCT ($2 \times 1.3\,mm^2$, 10 μm/pixel) and H&E section of in normal and septic rabbit tracheas: Normal trachea by OCT (**A**) and H&E (**B**); In contrast to normal tracheas, mucosal and submucosal edema is observed in the septic trachea by OCT (**C**) and H&E (**D**); Arrows indicate difference of tissue thickness/swelling between normal and septic rabbit tracheas (A,C). [Figure can be viewed in color online via www.interscience.wiley.com.]

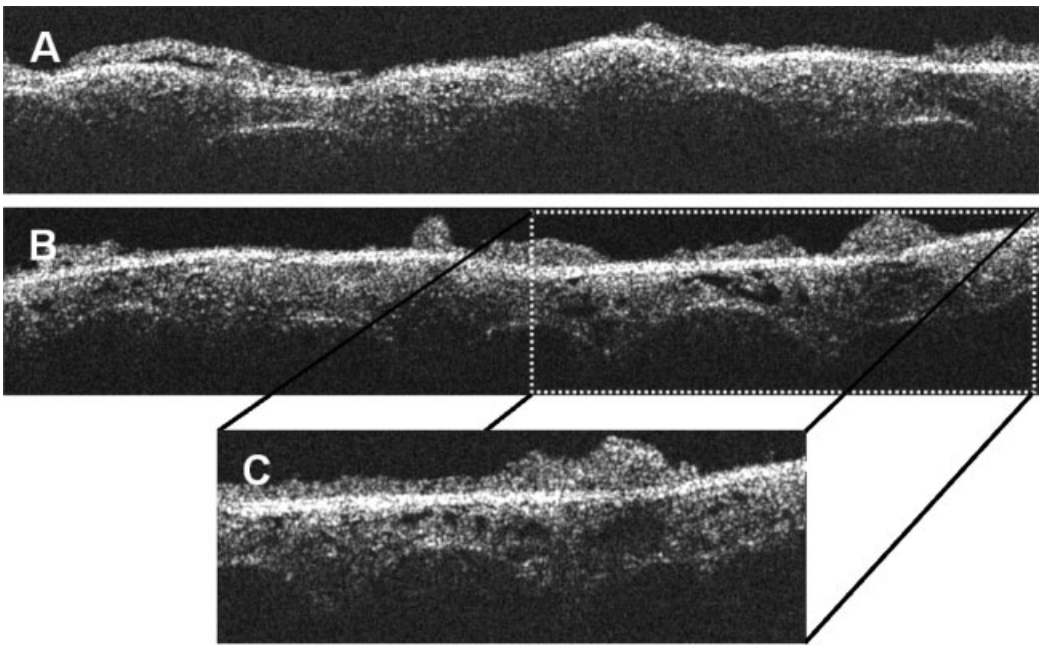

Fig. 6. In vitro flexible fiberoptic endoscopic OCT images of septic rabbit trachea: (**A**, **B**) were obtained at different stages of infection ($8 \times 1.3\ mm^2$, 10 μm/pixel); (**C**) higher magnification view of (B). The size of OCT image is $4 \times 1.3\ mm^2$ with 10 μm/pixel. Similar to Figure 4, the septic tracheal specimens showed marked edema and swelling of the submucosal region, with observed glandular structures.

Figure 6C shows a higher magnification image of Figure 6B. Similar to Figure 4, the septic tracheal specimens showed marked edema and swelling of the submucosal region, with glandular structures.

Figure 6 shows the ability of our OCT system to obtain high-resolution images even under extremely challenging conditions such as intubation. Similar structural information was previously obtained with the moving stage system, but contrast was lower because the image was acquired through the wall of an endotracheal tube, leading to boundary loss from tube walls. Another cause of lower contrast with the endoscopic OCT system is that the image was captured in a region beyond the fixed lens focal point because of the added thickness of the endotracheal tube. However, despite the highly challenging conditions under which this image was acquired, the endoscopic OCT image still has adequate resolution to distinguish edema formation in the septic trachea similar to that seen in Figure 4. In clinical practice, the bronchoscopist would not image through the wall of the endotracheal tube, but would pass the probe through the bronchoscope and image the mucosa directly.

DISCUSSION

Flexible fiberoptic bronchoscopy is a very commonly used procedure for diagnosis and treatment of pulmonary disease. There are a variety of medical conditions for which fiberoptic bronchoscopy is needed including primary and metastatic endobronchial malignancies, infectious and granulomatous diseases including mycobacterial and fungal infections, sarcoidosis, environmental exposures, and hypersensitivity reactions. Flexible fiberoptic bronchoscopy is usually performed under "white light" conditions. When a pathologic diagnosis is needed, biopsies are obtained by forceps through the 1–2 mm diameter working channel of the scope. Methods for selecting the location of the biopsies include visual inspection and radiologic localization. The diagnostic yield for biopsy specimens is variable due to depth and location of the abnormalities, degree of visible changes, and sampling error. Only a limited number of specimens can be obtained from the airway and biopsies may be associated with bleeding (and pneumothorax), limiting diagnostic accuracy, while increasing risk and expense. The depth range of OCT is sufficient to penetrate through the upper layers of exposed tissues on airway surfaces (maximal depth average 2–3 mm), where many endobronchial and pleural carcinomas originate or spread, and sufficient to detect many infectious or granulomatous diseases, and is equivalent to the depth that standard endobronchial forceps can sample. Thus OCT could potentially be of considerable value in assisting endobronchial diagnostics and help in guiding biopsy sites.

This animal study demonstrates that OCT is capable of imaging normal tracheal mucosal and submucosal micro-structural components including epithelium, lamina propria, submucosa, and cartilage, as well as detecting superficial airway pathology such as edema and swelling due to sepsis. OCT imaging had the capacity to detect differences in tracheal mucosal thickening between the normal control and septic groups of animals.

Given the impressive real-time tissue resolution, flexible fiberoptic bronchoscopic compatibility, and relatively inexpensive optical components, OCT has the potential to become a powerful tool in diagnostic pulmonary medicine. The micrometer scale resolution of OCT produces images that in the future may approach that of conventional "gold standard" histology. Flexible fiberoptic probes with rapid acquisition and processing of images will now enable in situ measurements to be performed. H&E processing for histologic diagnosis may artifactually desiccate the mucosal edema that occurs in some airway injury states, whereas OCT may obtain more accurate imaging. Some additional discrepancies between OCT and standard histology may be due to the fact that the two methodologies examine different tissue properties—optical reflectivity in OCT versus dye absorption in H&E staining.

Future research is needed in the areas of improving resolution to levels capable of visualizing individual cells and nuclei to distinguish benign from malignant lesions, optimizing methods for integration of OCT with bronchoscopes, and clinical correlation for detection of pathologic tissue changes in various respiratory diseases.

CONCLUSIONS

This study using excised normal and septic rabbit tracheas showed that OCT can distinguish many histologic features, usually requiring biopsy. Notable differences between normal and septic trachea were detected by OCT. This study suggests that OCT may be valuable for evaluating airway pathology in situ with high-resolution and useful in endoscopic applications.

ACKNOWLEDGMENTS

The authors thank David S. Mukai, and Naglaa E. Abbadi for expertise and technical support in histological evaluation. We also thank Dr. Ron Walton, Dr. Andre Yershov, and Dr. Brian Jordan at the U.S. Army Institute of Surgical Research, San Antonio, for the septic tracheal specimens.

REFERENCES

1. Tearney GJ, Brezinski ME, Bouma BE, Boppart SA, Pitris C, Southern JF, Fusimoto JG. In vivo endoscopic optical biopsy with optical coherence tomography. Science 1997;276:2037–2039.
2. Bouma BE, Tearney GJ. Power-efficient nonreciprocal interferometer and linear-scanning fiber-optic catheter for optical coherence tomography. Opt Letters 1999;24:531–533.
3. Rollins AM, Ung-arunyawee R, Chak A, Wong RCK, Kobayashi K, Sivak MV, Izatt JA. Real-time in vivo imaging of human gastrointestinal ultrastructure using endoscopic optical coherence tomography with a novel efficient interferometer design. Opt Letters 1999;24:1358–1360.
4. Hee MR, Izatt JA, Swanson EA. Optical coherence tomography of the human retina. Arch Ophthalmol 1995;113:325–332.
5. Bouma BE, Tearney GJ, Compton CC, Nishioka NS. High-resolution imaging of the human esophagus and stomach in vivo using optical coherence tomography. Gastrointest Endosc 2000;51:467–474.

6. Sivak MV, Kobayashi K, Izatt JA, Rollins AM, Ung-Runyawee R, Chak A, Wong RC, Isenberg GA, Willis J. High-resolution endoscopic imaging of the GI tract using optical coherence tomography. Gastrointest Endosc 2000;51: 474–479.
7. Tearney GJ, Jang IK, Kang DH, Aretz HT, Houser SL, Brady TJ, Schlendorf K, Shishkov M, Bouma BE. Porcine coronary artery imaging in vivo by optical coherence tomography. Acta Cardiologica 2000;55:233–237.
8. Kobayashi K, Izatt JA, Kulkarni MD, Willis J, Sivak MV. High-resolution cross-sectional imaging of the gastrointestinal tract using optical coherence tomography: preliminary results. Gastrointest Endosc 1998;47: 515–523.
9. Yelbuz TM, Choma MA, Thrane L, Kirby ML, Izatt JA. Optical coherence tomography: A new high-resolution imaging technology to study cardiac development in chick embryos. Circulation 2002;106:2771–2774.
10. Tearney GJ, Brezinski ME, Southern JF, Bouma BE, Boppart SA, Fujimoto JG. Optical biopsy in human urologic tissue using optical coherence tomography. J Urol 1997;157: 1915–1919.
11. Tearney GJ, Boppart SA, Bouma BE, Brezinski ME, Weissman NJ, Southern JF, Fujimoto JG. Scanning single-mode fiber optic catheter-endoscope for optical coherence tomography. Opt Letters 1996;21:543–545.
12. Tearney GJ, Bouma BE, Fujimoto FG. High-speed phase- and group-delay scanning with a grating-based phase control delay line. Opt Letters 1997;22:1811–1813.
13. Rollins AM, Kulkarnis MD, Yazdanfar S, Ung-arunyawee R, Izatt JA. In vivo video rate optical coherence tomography. Opt Express 1998;3:219–229.